Development and Testing of Ni-Cu Bimetallic Catalysts for Effective Syngas Production via Low-Temperature Methane Steam Reforming

Khzouz, M., Fakhim, B., Babaa, S., Ghaleeh, M., Sher, F. & Gkanas, E.

DOI 10.35702/catalres.1004
ISSN 2771-490X

Publisher: LIDSEN Publishing Inc.

CATALYSIS RESEARCH

Research Article

Development and Testing of Ni-Cu Bimetallic Catalysts for Effective Syngas Production via Low-Temperature Methane Steam Reforming

***Martin Khzouz*[1,2,*], *Babak Fakhim*[3], *Saleh Babaa*[2], *Mohammad Ghaleeh*[4], *Farooq Sher*[5], *Evangelos I Gkanas*[1,*]**

[1]Hydrogen for Mobility Lab, Centre for Advanced Low Carbon Propulsion Systems (C-ALPS), Coventry University, UK

[2]Department of Systems Engineering, Military Technological College, Muscat, Oman

[3]School of Aerospace, Mechanical and Mechatronic Engineering, The University of Sydney, Australia

[4]Department of Engineering, University of Northampton, Northampton, UK

[5]Department of Engineering, School of Science and Technology, Nottingham Trent University, Nottingham, UK

***Corresponding author:**

Martin Khzouz

Hydrogen for Mobility Lab, Centre for Advanced Low Carbon Propulsion Systems (C-ALPS), Coventry University. UK.
Email: marcin.khzouz@gmail.com

Evangelos I. Gkanas

Hydrogen for Mobility Lab, Centre for Advanced Low Carbon Propulsion Systems (C-ALPS), Coventry University. UK.
Email: ac1029@coventry.ac.uk

Received : November 02, 2022
Published : November 29, 2022

ABSTRACT

In the present work, novel bi-metallic catalysts for syngas production at low temperature steam reforming are developed, characterised and tested. Steam methane reforming by using bi-metallic Ni-Cu catalysts found to balance the product of CO to CO_2 ratios, while affected the water gas shift reaction by increasing the hydrogen selectivity up to 600°C. The addition of different amounts of Cu (3, 5, 7, 10 wt%) to the Ni catalyst for methane steam reforming showed different reactivity trends. One of the major outcomes of this work is the maximum load capacity of Cu (5wt.%Cu) to maintain the reactivity. For comparison purposes, mono-metallic catalysts of Cu and Ni were developed and tested along with the bi-metallic ones. The activity of the reaction decreased by doping more than 5wt.%Cu which affected the amount of hydrogen produced. This is related to the possible limited number of available sites required for hydrogen adsorption to maintain the reaction of methane steam reforming. Another important outcome of this work is the bi-metallic Ni-Cu catalysts did not decrease the amount of carbon formation.

Keywords: Bimetallic catalysts, steam methane reforming, Heterogeneous catalysts, syngas generation, Bimetallic Ni-Cu/Al_2O_3 catalyst.

INTRODUCTION

Steam-Methane Reforming(SMR) is considered to be the most financially viable technology for syngas production

[1]. Methane (CH_4) can be converted to syngas at elevated temperatures, normally above 800°C [2-4]. However, for the technology of Solid Oxide Fuel Cells (SOFCs), SMR at operating temperatures between 500-700°C is highly desirable, as the generated heat from the SOFCs can be utilised to increase the overall system efficiency [5,6]. The coupling of Methane steam reformers with SOFCs is already being used via combined heat and power (CHP) systems in residential stationary applications [7]. Residential CHPs use the established methane grid infrastructure, which facilitates the roll out of the Fuel Cell technology [7,8]. Over 120,000 CHP units have been sold and installed for domestic use in Japan by 2017 [9]. The fuels suitable to operate SOFCs come from a variety and mixture of gases including; H_2, CO and CH_4. The direct use of CH_4, results in the formation of coke at the anode and therefore negatively contributes towards the lifetime of the SOFCs. Therefore, external reforming at comparable temperatures to the operational SOFC temperatures in order to produce syngas has attracted attention for its benefit on SOFCs lifetime with negligible efficiency cost [10, 11].

The overall chemical reaction for methane steam reforming is described in Eq. 1. The reaction from Eq.1 is the result of the combination of the two reactions introduced in Eq. 2 (endothermic SMR) and Eq. 3 (exothermic water gas shift (WGS) reaction).

$$CH_4 + 2H_2O \rightleftharpoons CO_2 + 4H_2 \quad , \Delta H°_{298} = +165 \text{ kJ/mol} \quad \text{(Eq. 1)}$$

$$CH_4 + H_2O \rightleftharpoons CO + 3H_2 \quad , \Delta H°_{298} = +206 \text{ kJ/mol} \quad \text{(Eq. 2)}$$

$$CO + H_2O \rightleftharpoons CO_2 + H_2 \quad , \Delta H°_{298} = -41 \text{ kJ/mol} \quad \text{(Eq. 3)}$$

The SMR reaction involves a heterogeneous catalyst. The catalyst is made from metal oxides, which is known as metal oxide catalysts such as; Ni, Pt and Pd. The main issue for metal oxide catalysts lies on the fact that they deactivate due to metal sintering and thermal degradation. In addition, such catalysts favour carbon formation. This causes instability for the catalytic reaction performance. Bi-metallic catalysts have been also suggested to enhance the catalytic reaction as compared to the mono-metallic catalysts [12]. Improving the catalyst composition by doping with binary metals has the potential to improve the reaction behaviour. Both the surface composition and the bimetallic particle size can affect the catalytic performance of the reaction. The ex-situ catalytic performance test provides an indication for catalytic performance such as; methane fuel conversion, catalytic activity and product selectivity, which are essential design parameters to build an external reformer technology.

The addition of metallic Cu within the Ni catalyst can enhance the reactivity of the decomposition reaction of the hydrocarbon fuel [13-18]. The metallic Cu has the potential to enhance the methane decomposition reaction. The increasing a small amount of Cu (0.01 wt.%, 0.1 wt.%, 0.5 wt.%) to Ni (0.5 wt.%) catalyst can improve the reaction activity [19]. However, the catalytic performance was found to decrease at 750°C, because of the aggregation of the active particles and carbon formation [16, 17]. The catalyst promoter has the potential to affect the ensemble size of metal [20-23]. For the methane decomposition reaction, substitution of Cu over Ni showed an improvement of the catalytic reaction stability at 500-900°C with maximum conversion of 54% at 700°C [24]. Moreover, the Cu addition to Ni/SiO_2 catalysts was investigated in terms of enhancement of the catalytic stability [25]. The performance of decomposition reaction when utilising the Ni-Cu catalyst was increased as compared to the usage of the Ni/SiO_2 catalyst [26]. Methane decomposition has been reported over un-supported bimetallic Ni-Cu catalyst [24, 27-33]. Mainly, it was reported that Cu decreased the carbon formation with an improvement in the catalytic activity at 600°C for methane decomposition reaction. Furthermore, suggested that shifting the Ni/Cu composition further towards higher Cu contents could improve the carbon tolerance [34].

The aim of the current work is to examine the stability effect when introducing Cu promoters in Ni-based catalysts at low metal loadings (less than 10 wt.%) for methane steam reforming purposes. The work further adds in the understanding of the effect of the Cu addition in terms of mitigation of Ni aggregation and the stability of the catalyst structure. In addition, the reduction of carbon formation during the reaction due to the doping is investigated. For that reason, an experimental approach in the synthesis, characterisation and testing of the Ni-based bimetallic catalysts for methane steam reforming applications is presented. Several loadings of metallic Cu (3, 5, 7, 10 wt%) are introduced and the effects of the methane conversion, water conversion, hydrogen production and carbon production are discussed. The catalysts are characterised after the methane steam reforming reaction by means of XRD, SEM-EDX, TGA and BET analysis. Finally, a carbon formation analysis is introduced, presented and analysed.

MATERIALS AND METHODS

Catalyst Preparation

The catalyst was prepared via an impregnation method. The

raw materials (Nickel(II) nitrate hexahydrate - $Ni(NO_3)_2 \cdot 6H_2O$ and Copper(II) nitrate trihydrate - $Cu(NO_3)_2 \cdot 3H_2O$) were purchased from Alfa Aesar. For the preparation of the mono-metallic catalysts, $Ni(NO_3)_2 \cdot 6H_2O$ and $Cu(NO_3)_2 \cdot 3H_2O$ were dissolved in ethanol along with magnetic stirring for 30min. For the case of the bi-metallic catalysts, an additional of 30 min of stirring after the $Ni(NO_3)_2 \cdot 6H_2O$ was discharged to the $Cu(NO_3)_2 \cdot 3H_2O$ solution took place. Finally, trilobe Al_2O_3 catalyst carriers (6g) purchased by Johnson Matthey added to the nitrate metal solution and mixed for 120 minutes using ultrasonic mixer at room temperature. Then, the metal supported catalyst left to dry at 100°C for 8 hours. Finally, the catalyst was calcined at 500°C (5°C/min) for 5 hours.

Catalyst Characterisation

A Philips XL-30 with LaB6 filament SEM fitted with an Oxford Instruments INCA Energy Dispersive X-ray Spectroscopy (EDS) system was used to study the catalyst morphology. In principle, an electron beam is scanned over the catalyst surface which will generate signals. The signals detection produces the image. The SEM apparatus uses a NordlysS camera which is able to produce images with minimal geometric distortion at a resolution of 1344x1024 pixels. The SEM captures adjusted angle from 15°-130° upon a 50x50 mm stage. The images were displayed and recorded using INCA software. The fitted EDS allowed the study of elemental composition of the scanned samples. The EDS provides quantitative analysis for elemental composition providing the elemental distribution across the scanned sample. The scanned samples were coated with gold before being introduced to the microscope chamber in order to make electrically insulating samples conducting. The external morphology of the samples was recorded in the range of 1 μm up to 100 μm and a two-dimensional image was displayed on the computer screen using INCA software. A sample of the catalyst (around 1.4 g) was introduced to Micrometrics ASAP 2010 analyser. The BET surface area was determined by using the data from the isotherms during physisorption with N_2. The measured static gas volume during adsorption process was used to develop physisorption isotherms in order to calculate the Brunauer–Emmett–Teller (BET) surface [35]. The measurements were carried out over approximately 1.4 g of catalyst sample using a Micrometrics ASAP 2010 analyser. Accelerated Surface Area and Porosimetry (ASAP) uses the static volumetric technique to determine surface area using N_2 physisorption isotherms at -196°C. The sorption measurements were conducted over the range of relative pressures from 0.01 to 0.99 during adsorption and the relative pressure was subsequently reduced to 0.14 during the desorption stage. For the XRD analysis, a Bruker D8 Advanced Diffractometer was used fitted with XRD database provided by ICDD. The powder obtained from the catalyst scanned using XRD at room temperature at angles between 30° to 90°, with a step size of 0.02° and CuKα radiation, λ=0.154 nm and K=0.9. The XRD patterns were matched and assigned according to the XRD database (PDF-4+2012) provided by International Centre for Diffraction Data (ICDD). The TGA analysis was performed using a NETZSCH TG 209 F1 instrument. An amount of the sample (20mg) introduced to the aluminium crucible. The carbon formed on the sample after the reaction is treated using air (50ml/min) by increasing the temperature (10°C/min) from 25°C to 900°C. The sample was introduced to the TGA instrument in an aluminium crucible that can resist a high increase in the temperature. During the TGA process carbon deposited on the sample in the reaction was removed from the catalyst by oxidation in air at a flow rate of 50 ml/min and heating the sample (20 mg) in the oven chamber from 25°C to 900°C at a ramp rate of 10°C/min. Then, the percentage mass changes with temperature were recorded. The measured mass loss by TGA is assumed as sum of complete metal oxidation to NiO and Cu_2O and carbon burn off. The calculation assumed that the catalyst was fully reduced before performing TGA. Then, the accumulated carbon in grams for the reaction duration was calculated.

Catalytic Activity Measurements

The catalytic reaction took place in the experimental apparatus shown in Fig.1. The prepared catalysts (quantity of 3g) of the prepared catalyst packed in the middle of the reactor furnace (50 mm bed height). The reactor (395 mm lenght) was made from 316L stainless steel with diameter of 10.9 mm and wall thickness 0.89 mm. Methane (99.99% purity) was supplied to the reactor tube using Brooks mass flowmeter at flow rate of 25 ml/ min. The reaction was carried out between 500-700°C. The steam was injected at a molar ratio of 3:1, generated from water passing through the pipe wrapped with trace heater (OMEGA). A pump (Cole Palmer) controlled the flowrate of water. When the operation stabilised, gas samples were withdrawn for analysis using Refinery Gas Analyser (Agilent 7890A) every 15 minutes for a total duration of four hours. The entire piping system was purged with N_2 before commencing the reaction. Then, hydrogen injected at a flow rate of 10 ml/min for catalyst reduction purposes. As reported previously, the assigned reduction temperature measured by temperature programmed reduction was (650°C for 10% Ni, 250°C for 10%

Cu, 350°C for 7% Cu - 3% Ni, 380°C for 5% Cu - 5% Ni, 425°C for 7% Ni - 3% Cu) [36]. The reduction was performed by increasing the temperature to the target value by 5°C/min and maintain the target temperature for 30 minutes. After that, the system was purged again with N_2.

Figure 1: Experimental apparatus used for catalytic reaction activity test

RESULTS

The effect of Cu content on the Ni-based catalytic reactivity

Methane and water conversions

Fuel conversion and the catalyst selectivity for syngas production were tested at several reaction temperatures. The methane fuel conversion when utilising both the Ni mono-metallic and the Ni-Cu bimetallic catalysts is presented in Fig 2. The bi-metallic catalysts revealed lower conversion at 500-550°C comparing to the Ni mono-metallic catalyst. SMR is an endothermic reaction and thus, it is activated while the temperature is increased. The catalytic reactivity of Ni-based mono-metallic catalysts is enhanced at the temperature range of 500-550°C. The catalytic reactivity at 600°C showed that a small loading with Cu (3%) could lead on a higher conversion rate than the mono-metallic Ni catalyst. The small amount of Cu could enhance the WGS reaction by consuming CO, while extra CO is generated from the steam methane reaction. Increasing the Cu content up to 5% and 7%, resulted in lower methane fuel conversion compared to the mono-metallic Ni catalyst. This behaviour is related to the reduction of the active metal site for the methane steam reforming reaction. The lower methane conversion for 5% Ni - 5% Cu and 3% Ni - 7% Cu catalysts in comparison to the 7% Ni - 3% Cu at 600°C is attributed to the fact that the conversion takes place on the Ni surface and, as seen in Fig. 3, the water consumption was higher for the case of 7% Ni - 3% Cu. For the case of the mono-metallic 10% Cu catalysts, the levels of methane conversion were very low, as presented in Table 1. According to those outcomes, Cu is responsible only for WGS after the SMR takes place. For higher temperatures (650-700°C), it can be observed from Fig. 3 that the water conversion had decreased or remained at similar levels, indicating that the steam is no longer the main contributor for the catalytic methane reaction. This behaviour appears because at elevated operating temperatures, the methane decomposition reaction and the reverse WGS reaction are dominating.

DOI: https://doi.org/10.35702/catalres.1004

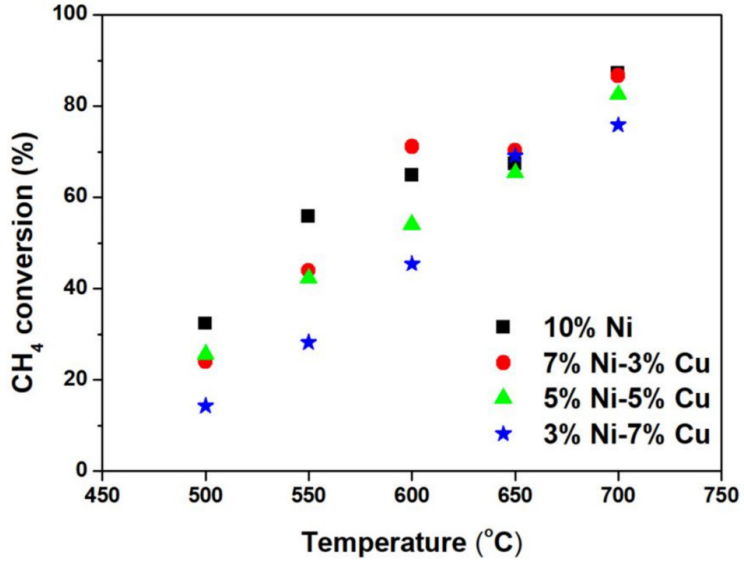

Figure 2: CH_4 conversion for the mono-metallic and the bi-metallic catalysts at various temperatures between 500-700°C

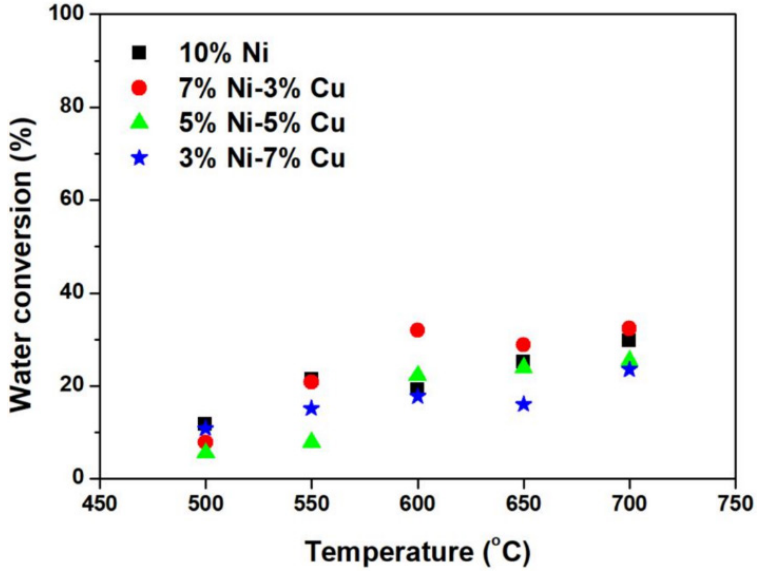

Figure 3: H_2O conversion for the mono-metallic and the bi-metallic catalysts at various temperatures between 500-700°C

Table 1. Activity of catalytic methane reaction for physically mixed monometallic 10% Cu and 10% Ni catalysts

	10%Cu	10%Ni, 10%Cu*	10%Ni, 10%Cu*	10%Ni, 10%Cu*
Temperature (°C)	700	700	600	500
S/C	3	3	3	3
CH_4 conversion (%)	9.7	87.0	55.8	28.6
Water conversion (%)	0.00	15.1	14.8	10.1
H_2 yield	0.08	2.19	1.56	0.87
CO_2 yield	0.01	0.23	0.24	0.17
CO yield	0.00	0.56	0.23	0.04

**Physical mixture of single metal (1.5 g of 10%Cu and 1.5 g of 10%Ni).*

Hydrogen yield

The hydrogen yield at the temperature range 500-700°C is presented in Fig 4. As extracted from Fig. 4, a common denominator for all the cases is an increase in the hydrogen yield with the increase of the reaction temperature. At the temperature range of 500-550°C, the mono-metallic Ni catalyst showed the highest hydrogen yield as compared to the performance of the bi-metallic catalysts. The large Ni content enhances the activation of C - H bonds for the SMR. At 600°C and for 7% Ni - 3% Cu, the hydrogen yield was 2.4 mol/mol-CH_4 and achieved the maximum value comparing to the other catalysts. This is mainly related to the WGS reaction. Hydrogen can be produced from both steam methane reforming over Ni and WGS reaction over active Cu. The catalyst becomes less selective to hydrogen at 500-600°C when more than 5 wt.% Cu is added to the catalyst. Thus, the low Ni content could reduce the fuel conversion and therefore the amount of H_2 produced. In addition, it was observed that the bimetallic catalyst has negligible effect on H_2 generated at 650-700°C, as the decomposition reaction is active at higher temperatures.

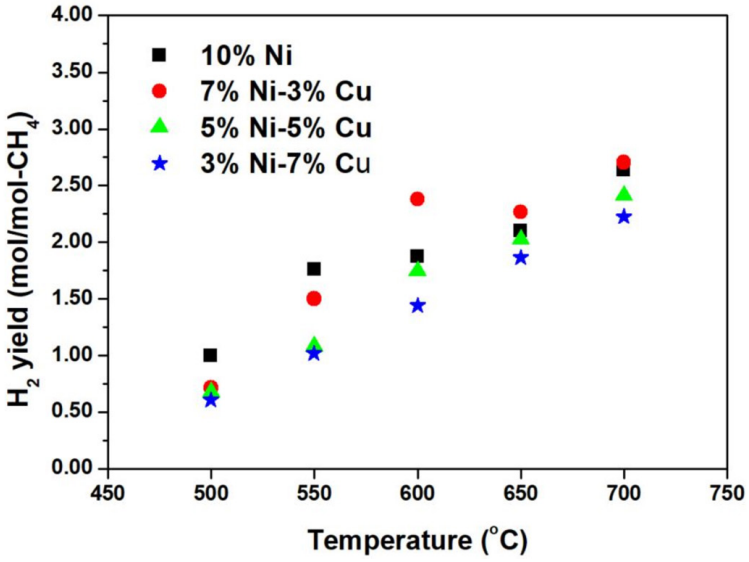

Figure 4: Hydrogen yield for the mono-metallic and the bi-metallic catalysts at various temperatures between 500-700°C

Carbon dioxide and carbon monoxide yields

The CO_2 yield for the mono-metallic and the bi-metallic catalysts at various temperatures between 500 – 700°C is presented in Fig. 5. The produced CO_2 is increasing for all the catalysts until 600°C, where the maximum CO_2 yield is achieved. After that point, when the reaction temperature reaches higher values (650-700°C) the CO_2 yield is decreasing. This is related to the nature of WGS reaction, which is less favourable under higher temperatures. The CO yield for the mono-metallic and the bi-metallic catalysts at various temperatures between 500 – 700°C is presented in Fig. 6. For all the studied catalysts, as the temperature increases, the CO yield also increases. In that case, CO is generated from both the SMR and the reverse WGS reaction. The CO yield at 500°C is very low for all the catalysts, as under these conditions, the WGS is the favourable reaction. The effect of Cu addition in the bi-metallic catalysts showed that the CO can produce by both the WGS reaction and SMR reaction [20-23]. For the case of 700°C, the Cu catalytic addition at high temperature encourages strongly the reverse WGS reaction, and as a result, a higher amount of CO is generated from the activated decomposition reaction.

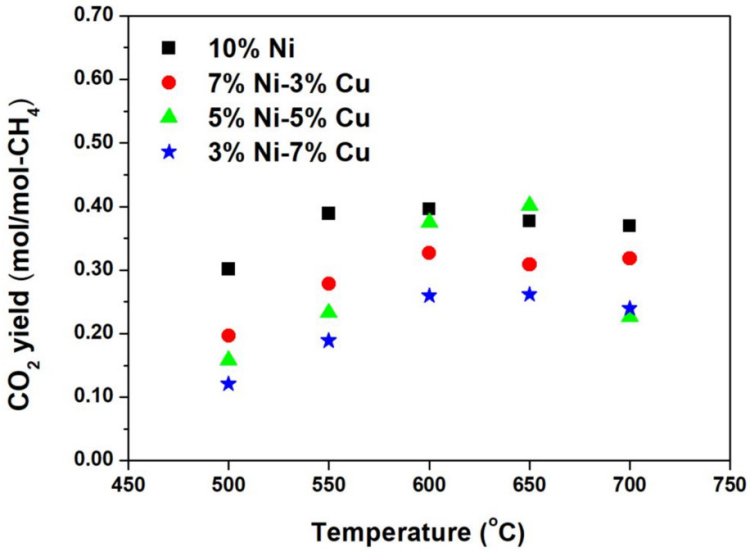

Figure 5: CO_2 yield for the mono-metallic and the bi-metallic catalysts at various temperatures between 500-700°C

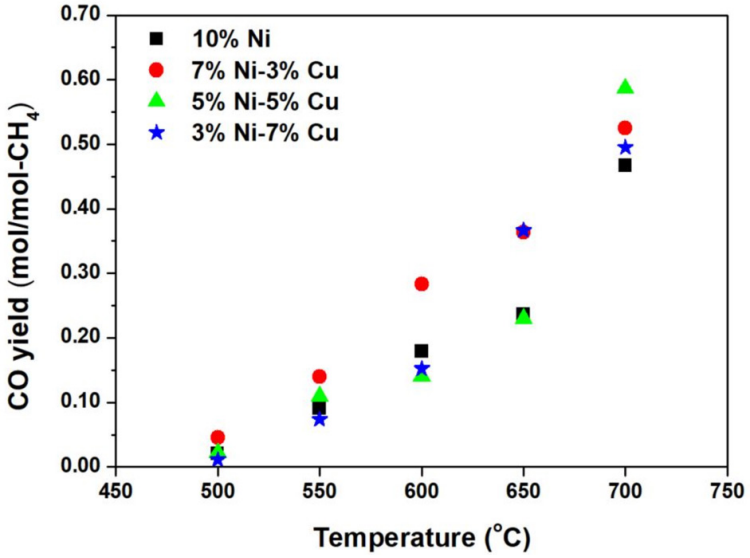

Figure 6: CO yield for the mono-metallic and the bi-metallic catalysts at various temperatures between 500-700°C

Steam methane reforming over monometallic mixture

The MSR was also studied over monometallic 10% Ni and 10% Cu catalysts. According to the data presented in Table 1, the mono-metallic 10% Cu catalyst at 700°C was able to achieve 9.7% CH_4 conversion. In addition, small traces of CO_2 were detected. In general, Cu is not an effective catalyst in terms of selection for methane steam reforming applications. The methane reaction mechanism occurs when derived intermediates of CH_4 are chemisorbed on the surface of the catalyst and react with the water species [37]. Cu catalyst normally doesn't activate the C-H bond necessary for SMR [38]. The main objective of SMR is to convert CH_4 to H_2 and CO, and then it reacts with steam to produce CO_2 and H_2. By physical mixing the two catalysts, 10%Ni and 10%Cu, an effective activity at 700°C was observed by achieving the highest CH_4 conversion. The 7% Ni - 3% Cu catalyst at 600°C showed 71.1% methane conversion and 2.4 mol H_2, which is higher than carrying the reaction over the physical mixture of the mono-metallic catalysts. The CO removal process via WGS reaction where further methane was converted via SMR to CO then to H_2 could be a reason. From the previous analysis, the CH_4 reaction was active at 650-700°C, a significant amount of H_2 and CO were developed inside the reactor. This kind of behaviour is related to the activation of the C-H bonds during the steam reforming reaction.

Characterization of reacted catalysts

SEM-EDX of the reacted catalysts

The SEM/EDX micrographs of the reacted catalysts at the minimum (500°C) and maximum (700°C) reaction temperatures are presented in Fig. 7 and Fig. 8 respectively. The EDX spectrum is used to detect the main composition on the catalyst surface. The monometallic 10% Ni catalyst reacted at 700°C showed a higher degree of agglomeration compared to the same reacted catalyst at lower temperature.

The 7% Ni - 3% Cu revealed shades of white and bright white spots. The agglomeration alongside the Al_2O^3 support plane were observed for the 5% Ni - 5% Cu catalysts at both reaction temperatures. The reacted 3% Ni-7% Cu catalyst operated at 500°C revealed changes and with increasing the operating temperature, more agglomeration was observed

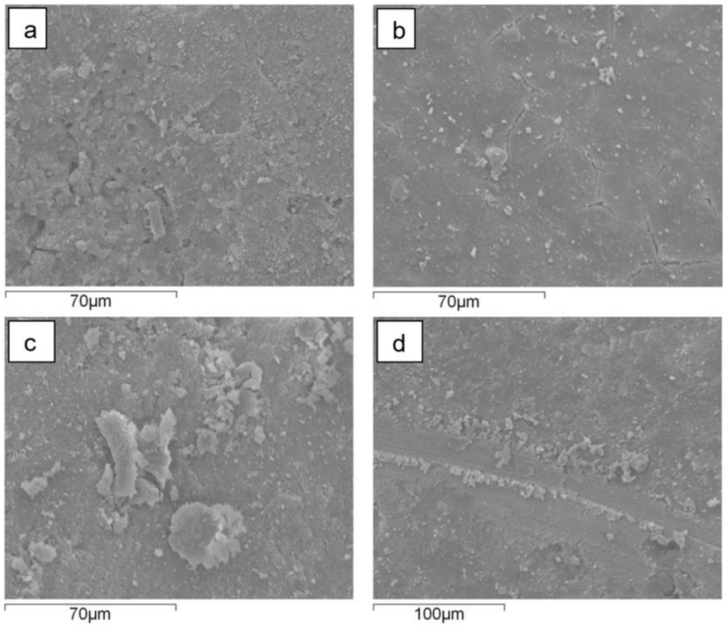

Figure 7: SEM micrographs for the studied catalysts at the lowest temperature (500°C) for a) the monometallic Ni catalyst, b) for the bimetallic 7%Ni – 3%Cu catalyst, c) for the bimetallic 5%Ni – 5%Cu catalyst and d) for the bimetallic 3%Ni – 7%Cu catalyst

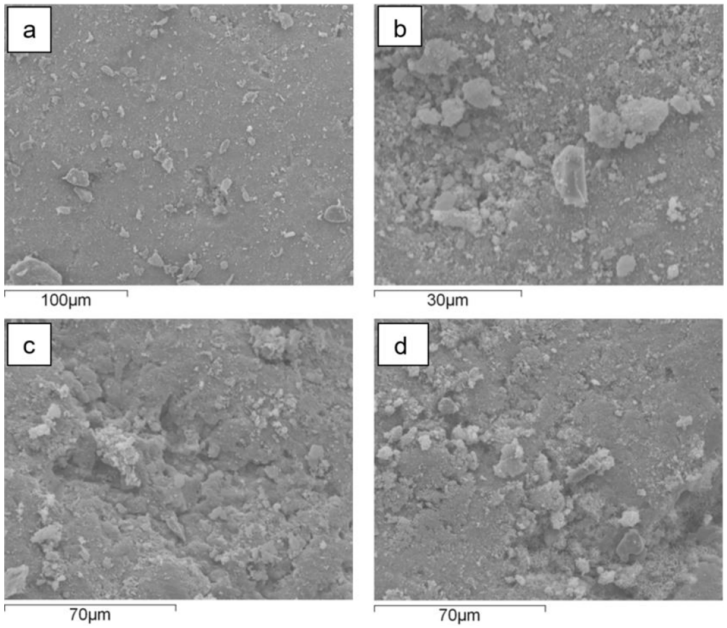

Figure 8: SEM micrographs for the studied catalysts at the highest temperature (700°C) for a) the monometallic Ni catalyst, b) for the bimetallic 7%Ni – 3%Cu catalyst, c) for the bimetallic 5%Ni – 5%Cu catalyst and d) for the bimetallic 3%Ni – 7%Cu catalyst

Surface area analysis

The surface area analysis for the as-prepared and the reacted catalysts (for the reaction temperatures 500 and 700°C) is presented in Table 2. The catalytic surface area of the reacted catalysts showed lower values, as compared with the surface area of the as prepared catalyst. The reacted catalysts presented a low N_2 volume of adsorption during the BET test. This is inferred to the pores blockage of the Al_2O_3 support, as agglomeration was observed from the SEM micrographs, resulting in reduced amount of nitrogen adsorbed during the test.

For the reacted catalysts at 700°C, both the mono-metallic 10%Ni and the bi-metallic 7%Ni-3%Cu revealed low surface area by comparing the results for the same reacted catalysts at 500°C. This is related to the fact that high operating temperature has a negative aspect on the catalyst surface area and the high Ni content at high temperature is active with methane steam reforming reaction due to thermodynamic nature of the reaction. On the other hand, the bi-metallic catalysts of 5% Ni - 5% Cu and 3% Ni -7% Cu showed lower surface area at 500°C than the same catalysts reacted at 700°C. The large Cu content is engaged with high activity for WGS reaction at low temperature, leading to the support pore coverage and as a result, to deactivation.

Table 2. The surface area of fresh and tested catalysts at 500°C and 700°C

	10%Ni	7%Ni-3%Cu	5%Ni-5%Cu	3%Ni-7%Cu
Surface area, fresh (m^2/g)	122	125	128	125
Surface area, reacted at 500°C (m^2/g)	93.3	97.1	93.2	91.7
Surface area, reacted at 700°C (m^2/g)	86.1	89.0	95.0	100
Pore diameter, fresh (nm)	19.9	19.8	19.6	20.1
Pore diameter, reacted at 500°C (nm)	20.1	18.3	20.1	20.5
Pore diameter, reacted at 700°C (nm)	21.9	19.8	18.4	16.1

XRD analysis

The XRD analysis of the reacted catalysts were analysed by the commercial software Match3! and the databases from FullProf Suite were utilised. Fig. 9 presents the X-ray diffraction patterns. The patterns for the mono-metallic 10%Ni catalyst and the bi metallic catalysts are presented for the reaction at 500°C in Fig. 9a, where the peaks are matched to the Ni, Cu, CuNi and Al_2O_3. The phase Al_2O_3 originates from the Al support used. The patterns for the same catalysts for the reaction at 700°C are presented in Fig. 9b. Finally, the comparison between the patterns of the 7%Ni-3%Cu catalysts in two different temperatures, 500 and 700°C is presented in Fig. 9c. The metal crystallite stability is related to the metal interaction with the support and is directly proportional with the melting temperature of the active metal. Thus, crystallite growth was found when the reaction temperature was increased as indicated from the XRD patterns changes at 700°C, as compared with the XRD patterns at 500°C. The XRD patterns for the metallic Ni-phase is present at both 44° and 52°, and by utilising the Scherrer equation, the average Ni crystallite size was 17.4 nm. In addition, for the case of the 7%Ni-3%Cu catalyst, the peaks for Ni and Cu are also shifted to higher angles as the temperature increases, indicating the presence of internal stresses in the material. Finally, at 700°C, the presence of an extra peak of Al_2O_3 at $2\theta=48°$ has been identified. The reacted bimetallic catalysts revealed patterns matched to Ni, Cu and Ni-Cu phases.

DOI: https://doi.org/10.35702/catalres.1004

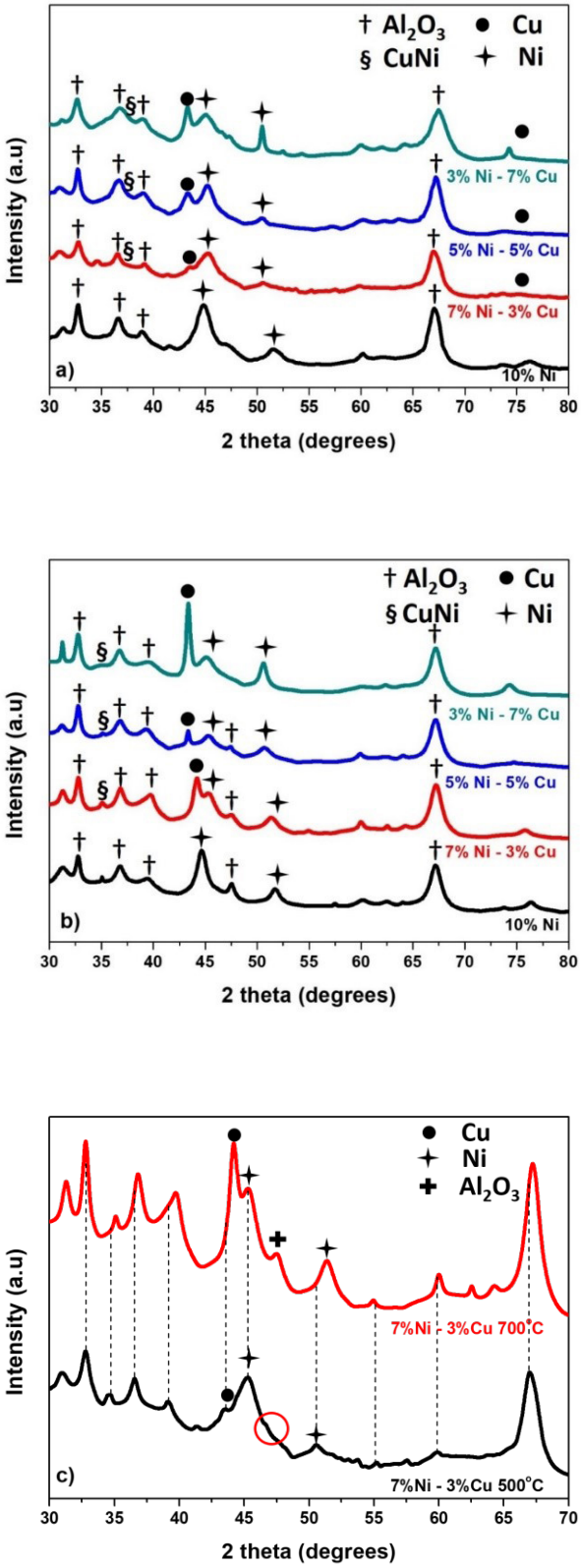

Figure 9: X-ray diffraction for tested catalysts at 500°C (9a) and at 700°C (9b). Finally, the diffraction patterns for the catalyst 7%Ni-3%Cu at 500°C and 700°C are presented (9c).

DOI: https://doi.org/10.35702/catalres.1004

Carbon formation for reacted catalysts

Carbon is formed during the catalytic reaction on the catalyst surface due to the absorption of hydrocarbon species and hydrogen release [39]. The carbon formation is mainly produced from the CO decomposition (Eq. 4), the CH_4 decomposition or a CH_4 dehydrogenation reaction (Eq. 5) and the CO reduction (Eq. 6). The catalyst selectivity for solid carbon (SelC) was estimated as shown in Eq. 7.

$2CO \rightleftharpoons C + CO_2$, $\Delta H°_{298}$ = -172 kJ/mol (Eq. 4)

$CH_4 \rightleftharpoons C + 2H_2$, $\Delta H°_{298}$ = +75 kJ/mol (Eq. 5)

$CO + H_2 \rightleftharpoons C + H_2O$, $\Delta H°_{298}$ = -131 kJ/mol (Eq. 6)

$$Sel_C\ (\%) = 100 \times \frac{n_{carbon}}{n_{CH_4,in}} \quad \text{(Eq.7)}$$

Out of the thermodynamic point of view, the forward reaction of CH4 decomposition (Eq. 5) is favoured at the temperatures 600-750°C while the opposite effect occurs for the reactions described by Eq.4 and Eq.6 at the same temperature range as shown in Fig.10. The role of the catalyst is to have a sufficient activity to counterbalance the coke deposition. The effect of bimetallic catalyst is observed from carbon formation analysis presented in Fig.11. It is difficult to detect a uniform trend, as several reactions can occur at the temperature range that the reactions took place. The amount of carbon formed when using bi-metallic catalysts was in general larger than the monometallic 10%Ni catalyst. The 10%Ni catalyst prepared in the present work showed sufficient stability, in terms of carbon formation when comparing it with Ni-Cu catalysts. Bimetallic catalysts did not find to decrease the carbon formation. The Ni dilution with small amount of Cu suggest that unstable carbide intermediated formed during the reaction and remained on the metal surface and later on the carbide was decomposed forming the carbon on the catalyst surface. The current prepared bimetallic catalyst did not improve the carbon tolerance compared with 10%Ni catalyst. It might be that a higher carbon deposition is formed as larger metal particles are formed from dilution of Ni with Cu as indicated from BET and XRD analysis.

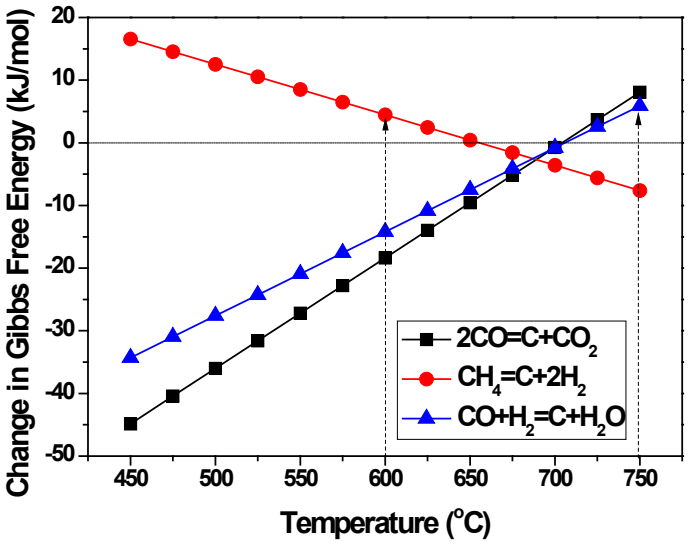

Figure 10: Gibbs free energy for carbon formation reactions at temperature 450-750°C

DOI: https://doi.org/10.35702/catalres.1004

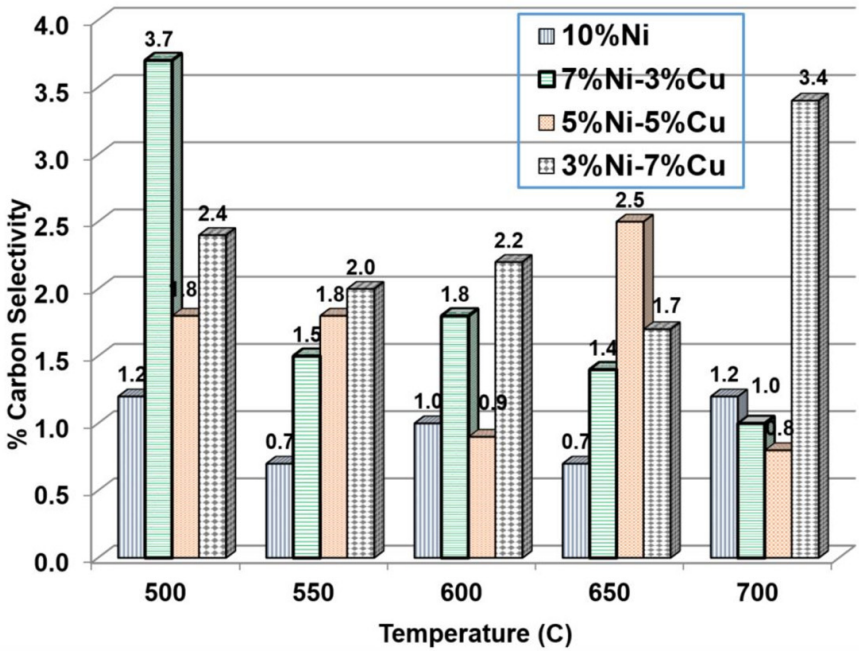

Figure 11: Selectivity of carbon formation for the tested mono-metallic and bi-metallic catalysts at all the studied temperatures (500-700°C)

CONCLUSIONS

In this work, various bi-metallic catalysts based on Ni and Cu were developed, characterised and tested under various temperatures in the range of 500-700°C. For comparison purposes, mono-metallic catalysts of Ni and Cu were prepared and tested. All the catalysts were tested regarding their behaviour for methane steam reforming reaction. The loadings considered for the bi-metallic catalysts were 10, 7, 5, and 3%wt. The maximum conversion value (87%) was obtained at the maximum temperature of 700°C for the case of the mono-metallic catalyst (10%Ni). The results showed an increasing amount of CO produced when the reaction temperature was increased due to the reverse WGS and methane decomposition. The bimetallic catalysts improved the catalyst selectivity for WGS reaction at the lower temperatures between 500 – 600°C. The bi-metallic catalyst with the small amount of Cu (3wt.%) showed good conversion of fuel at 600°C, where the catalyst revealed 71.1% methane conversion and 2.4 mol hydrogen were produced. The prepared bi-metallic catalysts did not find to decrease the carbon formation. The 10%Ni catalyst prepared on this study showed good stability regarding carbon formation compared to the prepared bimetallic Ni-Cu catalysts.

REFERENCES

1. Schröders S, Verfondern K, Allelein HJ. (2018). Energy economic evaluation of solar and nuclear driven steam methane reforming processes. Nuclear Engineering and Design. 329:234-246.

2. Lee FB. (2001). A comparative study of fuels for on-board hydrogen production for fuel-cell-powered automobiles. International Journal of Hydrogen Energy. 26(4):381-397.

3. Navarro RM, Peña MA, Fierro JLG. (2007). Hydrogen production reactions from carbon feedstocks: Fossil fuels and biomass. Chem Rev. 107(10):3952-3991.

4. Steinberg M. (1998). Production of hydrogen and methanol from natural gas with reduced CO_2 emission. International Journal of Hydrogen Energy. 23(6):419-425.

5. Roh H-S, Jun K-W. (2009). Low temperature methane steam reforming for hydrogen production for fuel cells. Bull Korean Chem Soc. 3(1):153-156.

6. Khzouz M, Gkanas E. (2017). Experimental and Numerical Study of Low Temperature Methane Steam Reforming for Hydrogen Production. Catalysts. 8(1):5.

7. Hou Q, Zhao H, Yang X. (2018). Thermodynamic performance study of the integrated MR-SOFC-CCHP system. Energy. 150:434-450.

8. Irving PM, Pickles JS. (2007). Operational requirements for a multi-fuel processor that generates hydrogen from Bio- and petroleum-based fuels for both SOFC and PEM fuel cells. ECS Transactions. 5:665-671.

9. Ramadhani F, Hussain MA, Mokhlis H, Hajimolana S. (2017). Optimization strategies for Solid Oxide Fuel Cell (SOFC) application: A literature survey. Renewable and Sustainable Energy Reviews.76:460-484.

10. Zhang X, Chan SH, Li G, Ho HK, Li J, Feng Z. (2010). A review of integration strategies for solid oxide fuel cells. Journal of Power Sources. 195(3):685-702.

11. Huang Y-L, Hussain AM, Wachsman ED. (2018). Nanoscale Cathode Modification for High Performance and Stable Low-Temperature Solid Oxide Fuel Cells (SOFCs). Nano Energy. 49:186-192.

12. Polychronopoulou K, Charisiou N, Papageridis K, Sebastian V, Hinder S, Dabbawala A, et al. (2018). The effect of Ni addition onto a Cu-based ternary support on the H2 production over glycerol steam reforming reaction. Nanomaterials. 8(11):931.

13. Wu H, La Parola V, Pantaleo G, Puleo F, Venezia A, Liotta L. (2013). Ni-Based Catalysts for Low Temperature Methane Steam Reforming: Recent Results on Ni-Au and Comparison with Other Bi-Metallic Systems. Catalysts. 3(2):563-583.

14. Angeli SD, Monteleone G, Giaconia A, Lemonidou AA. (2014). State of the art catalysts for CH_4 steam reforming at low temperature. International Journal of Hydrogen Energy. 39(5):1979-1997.

15. De Rogatis L, Montini T, Cognigni A, Olivi L, Fornasiero P. (2009). Methane partial oxidation on NiCu-based catalysts. Catalysis Today. 145(1-2):176-185.

16. Li J, Gong Y, Chen C, Hou J, Yue L, Fu X, et al. (2017). Evolution of the Ni-Cu-SiO_2 catalyst for methane decomposition to prepare hydrogen. Fusion Engineering and Design. 125:593-602.

17. Li J, Zhao L, He J, Dong L, Xiong L, Du Y, et al. (2016). Methane decomposition over high-loaded Ni-Cu-SiO2 catalysts. Fusion Engineering and Design. 113:279-287.

18. Khzouz M, Wood J, Pollet B, Bujalski W. (2013). Characterization and activity test of commercial Ni/Al_2O_3, Cu/ZnO/Al_2O_3 and prepared Ni–Cu/Al_2O_3 catalysts for hydrogen production from methane and methanol fuels. International Journal of Hydrogen Energy. 38(6): 1664-1675.

19. Huang T-J, Yu T-C, Jhao S-Y. (2005). Weighting variation of water–gas shift in steam reforming of methane over supported Ni and Ni–Cu catalysts. Industrial & Engineering Chemistry Research. 45(1):150-156.

20. Rostrup-Nielsen JR. (1984). Sulfur-passivated nickel catalysts for carbon-free steam reforming of methane. Journal of Catalysis. 85(1):31-43.

21. Andersen NT, Topsøe F, Alstrup I, Rostrup-Nielsen JR. (1987). Statistical models for ensemble control by alloying and poisoning of catalysts: I. Mathematical assumptions and derivations. Journal of Catalysis. 104(2):454-465.

22. Nishiyama Y, Tamai Y. (1974). Carbon formation on copper-nickel alloys from benzene. Journal of Catalysis. 33(1): 98-107.

23. Ponec V. (1983). Catalysis by alloys in hydrocarbon reactions. In: D.D. Eley HP, Paul BW, editors. Advances in Catalysis: Academic Press. P:149-214.

24. Chen J, Li Y, Li Z, Zhang X. (2004). Production of COx-free hydrogen and nanocarbon by direct decomposition of undiluted methane on Ni–Cu–alumina catalysts. Applied Catalysis A: General. 269(1-2):179-186.

25. Takenaka S, Shigeta Y, Tanabe E, Otsuka K. (2003). Methane decomposition into hydrogen and carbon nanofibers over supported Pd–Ni catalysts. Journal of Catalysis. 220(2):468-477.

26. Li Y, Chen J, Qin Y, Chang L. (2000). Simultaneous production of hydrogen and nanocarbon from decomposition of methane on a nickel-based catalyst. Energy & Fuels. 14(6):1188-1194.

27. Echegoyen Y, Suelves I, Lázaro MJ, Sanjuán ML, Moliner R. (2007). Thermo catalytic decomposition of methane over Ni–Mg and Ni–Cu–Mg catalysts: Effect of catalyst preparation method. Applied Catalysis A: General. 333(2): 229-237.

28. Echegoyen Y, Suelves I, Lázaro MJ, Moliner R, Palacios JM. (2007). Hydrogen production by thermocatalytic decomposition of methane over Ni-Al and Ni-Cu-Al catalysts: Effect of calcination temperature. Journal of Power Sources. 169(1):150-157.

29. Lázaro MJ, Echegoyen Y, Suelves I, Palacios JM, Moliner R. (2007). Decomposition of methane over Ni-SiO_2 and Ni-Cu-SiO_2 catalysts: Effect of catalyst preparation method. Applied Catalysis A: General. 329:22-29.

30. Suelves I, Lázaro MJ, Moliner R, Echegoyen Y, Palacios JM. (2006). Characterization of NiAl and NiCuAl catalysts prepared by different methods for hydrogen production by thermo catalytic decomposition of methane. Catalysis Today. 116(3):271-280.

31. Moliner R, Echegoyen Y, Suelves I, Lázaro MJ, Palacios JM. (2008). Ni–Mg and Ni–Cu–Mg catalysts for simultaneous production of hydrogen and carbon nanofibers: The effect of calcination temperature. International Journal of Hydrogen Energy. 33(6):1719-1728.

32. Li J, Lu G, Li K, Wang W. (2004). Active Nb_2O_5-supported nickel and nickel–copper catalysts for methane decomposition to hydrogen and filamentous carbon. Journal of Molecular Catalysis A: Chemical. 221(1-2):105-112.

33. Wang H, Baker RTK. (2004). Decomposition of methane over a Ni–Cu–MgO catalyst to produce hydrogen and carbon nanofibers. J Phys Chem. 108(52):20273-20277.

34. Götsch T, Schachinger T, Stöger-Pollach M, Kaindl R, Penner S. (2017). Carbon tolerance of Ni–Cu and Ni–Cu/YSZ sub-µm sized SOFC thin film model systems. Applied Surface Science. 402:1-11.

35. Brunauer S, Emmett PH, Teller E. (1938). Adsorption of gases in multimolecular layers. J Am Chem Soc. Contribution from the bureau of chemistry and soils and george washington university. 60(2):309–319.

36. Khzouz M, Gkanas EI, Du S, Wood J. (2018). Catalytic performance of Ni-Cu/Al_2O_3 for effective syngas production by methanol steam reforming. Fuel. 232:672-683.

37. Wei J, Iglesia E. (2004). Isotopic and kinetic assessment of the mechanism of reactions of CH_4 with CO_2 or H_2O to form synthesis gas and carbon on nickel catalysts. Journal of Catalysis. 224(2):370-383.

38. Wei J, Iglesia E. (2004). Structural requirements and reaction pathways in methane activation and chemical conversion catalyzed by rhodium. Journal of Catalysis. 225(1):116-127.

39. Bengaard HS, Nørskov JK, Sehested J, Clausen BS, Nielsen LP, Molenbroek AM, et al. (2002). Steam Reforming and Graphite Formation on Ni Catalysts. Journal of Catalysis. 209(2):365-384.

Citation: Khzouz M, Gkanas EI, et al. (2022). Development and Testing of Ni-Cu Bimetallic Catalysts for Effective Syngas Production via Low-Temperature Methane Steam Reforming. Catalysis Research. 2(1):4.

DOI: https://doi.org/10.35702/catalres.1004